Preliminary Study of Bead-On-Plate Welding Bead Geometry for 316L Stainless Steel Using GMAW

Huifeng Wang
PhD Student
Charles Darwin University
Faculty of Science and Technology
Australia

Stefanija Klaric
Associate Professor
Charles Darwin University
Faculty of Science and Technology
Australia

Sara Havrlišan
Assistant Professor
University of Slavonski Brod
Mechanical Engineering Faculty of Slavonski Brod
Croatia

The application of the gas metal arc welding (GMAW) process can produce metal parts in additive manufacturing (AM) and has the advantages of fast production speed and material saving. There are some different requirements for welding beads between the AM process and the usually welded joints, so preliminary research on the 316L GMAW is conducted to find the optimal voltage, wire feed speed (WFS), and travel speed (TS). Taguchi algorithm was used firstly to obtain parameters to achieve the desired higher reinforcement, lower width, and higher aspect ratio (R/W). The voltage of 19 V, WFS of 500 cm/min, and TS of 15 cm/min were obtained as the optimal one among the samples. To further investigate the influence of the parameters and verify the result, a two-factor- three-level full factorial design was carried out, with the consideration of the interaction between factors. At last, the studied parameters were used in the AM process using a GMAW welding robot to verify the reliability.

Keywords: *gas metal arc welding (GMAW), travel speed (TS), wire feed speed (WFS), Taguchi method, design of experiment (DOE)*

1. INTRODUCTION

Additive manufacturing (AM), which in principle manufactures products layer by layer developed rapidly during the last decades because of its advantages such as high productivity, low cost, and high material utilization rate [1-6]. Wire + arc additive manufacturing (WAAM) is one important type of AM method, during which metal wires, such as titanium, nickel, and stainless steel [7, 8], melt, and deposit on a substrate to manufacture the product [9]. Furthermore, welding processes that can be applied for WAAM include gas metal arc welding (GMAW), gas tungsten arc welding (GTAW), and plasma arc welding (PAW). Among them, GMAW showed its advantages like higher deposition rate in the fabrication of thin multi-walled structures with minimum capital cost [10, 11]. Regarding the materials used in GMAW AM, stainless steel is widely used in the fields of construction, ocean, chemical industry, and papermaking because of its good comprehensive performance and relatively low price [12]. Therefore, 316L stainless steel will be selected as the additive material in the following research.

During the GMAW process, welding parameters can significantly affect the forming morphology and geometric dimensions of the deposited pass [13]. The forming morphology of the deposition has an important impact not only on the internal defects of additive components, such as slag inclusions, porosities, cracks, etc., but also on manufacturing productivity. Therefore, it is necessary to conduct in-depth research on the effects of process parameters on the forming morphology and geometric dimensions of single-pass deposition [14].

Many factors affect the morphology and geometric dimensions of single-pass deposition, such as wire feeding speed (WFS), travel speed (TS), shielding gas composition and flow rate, elongation of the welding wire, etc. [11, 14, 15]. The influence of GMAW welding parameters on weld bead geometry and mechanical properties has been studied by many researchers and some of them aim to use the results in the following AM process. I.M.W Ekaputra et al. [16] applied different welding speeds (175 mm/min, 190 mm/min, 205 mm/min) and voltage of 20.1 V in their study for SS 316L. The results revealed that there was no significant difference in hardness in the weld metal zone (WM) under different welding speeds, while the welding speed of 175 mm/min can bring a higher tensile and yield strength. In the study of Manas Kumar Saha et al. [17], welding current (120-220 A), voltage (22-30 V), and TS (6.0-7.0 mm/s) were applied, and austenite stainless steel (316) weld beads were formed on low alloy structural steel (E350) by GMAW. The results showed that the application of higher heat input resulted in larger bead width, lower reinforcement, and lower penetration.

In the optimization of the welding parameters, different methodologies can be applied. For example, Vora et al. [13] applied Box-Behnken design (BBD) on 2.25 Cr-1.0 Mo steel GMAW process. Wire feed speed, travel speed, and voltage were chosen as the input parameters, and bead width and bead height were chosen as the output parameters. Based on the BBD results, a multi-objective teaching-learning-based optimization (MOTLBO) was applied to achieve max bead height and min bead width. Rakesh Chaudhari et al. applied the Respond surface BBD technique in their research, and bead height (BH) and bead width (BW) were selected as response variables [18]. Three factors and three levels

Received: August 2024, Accepted: September 2024
Correspondence to: Huifeng Wang, PhD Student
Charles Darwin University, Faculty of Science and Technology, Darwin, Australia
E-mail: huifeng.wang@students.cdu.edu.au
doi: 10.5937/fme2404563W

were selected, which were WFS (4 m/min, 5 m/min, and 6 m/min), TS (125 mm/min, 150 mm/min, and 175 mm/min) and voltage (19 V, 20 V, and 21 V). The following parameters (WFS of 5.50 m/min, TS of 141 mm/min, and voltage of 19 V) were applied in their AM process [19]. Ping Yao, et al. [20] used Taguchi and surface response method to find out the influence of different inclinations of welding torch (welding angle) on the appearance, width, reinforcement, and penetra–tion of welding beads under welding parameters as voltage (19.6 V), current (80 A) and TS (30 cm/min), and obtained that the optimal parameter setting was 70°. The genetic algorithm was applied by Kumar et al. to reveal the influence of process variables on the layer geometry of 304 SS [21]. Box-Behnken design (BBD) was applied on GMAW-based WAAM, and TS, voltage, and WFS were defined as the input parameters and the maximum bead height (BH) of 7.81 mm, and a minimum bead width (BW) of 4.73 mm was obtained by using the optimal parameters.

According to the above literature review, welding voltage, WFS, and TS are usually applied as the researched welding parameters in the research of GMAW weld bead geometry and mechanical properties. Although the ranges of parameters are similar, there are still differences in experimental results due to the differences in welding equipment, welding environment, or materials conditions. It is important to mention that due to the accumulative nature of the process, even the small differences in parameters and resulted geometry of individual layers can significantly influence the final product. Therefore, in this paper, the Taguchi method was applied first to obtain the suitable parameters' ranges, and then the full factorial design was used to get more optimal results, all with the aim of obtaining suitable parameters for better additive manufacturing products.

2. MATERIALS, EQUIPMENT, AND EXPERIMENT DESIGN

2.1 Experiment materials

The present study bead-on-plate trails will be carried out on Q235 carbon steel plate (100 × 30 × 5 mm). The 1.2 mm diameter ER316L metal core wire is utilized, which is provided by Sandvik, and the grade is 19.12.3. LSi. The composition of Q235 is C 0.2%, Si 0.35%, Mn 1.4%, P 0.045%, S 0.045%, Cr 0.3%, and Ni 0.3% [22]. The composition of 316L stainless (arc wire ER316L) is C 0.016%. Si 0.51%, Mn 2.14%, P0.013%, S 0.014%, Cr 18.96%, Cu 0.03%, Ni 12.73%, Mo 2.32% [23], and the rest is Fe.

2.2 Welding equipment and parameters

The experimental setup involved a FANUC Robot, R-30iB robot control cabinet, wire feeder, Lincoln welding power, and shielding gas cylinders (argon), as shown in Figure 1. The GMAW torch is installed in front of the robot arm. Fanuc iPendant is utilized as the operator interface device to display the software menus and control the welding robot.

In this study, 100% Argon will be employed for the product shield gas, and the gas flow will be 15 L/min. The distance between the torch and workpiece is 15 mm. Welding voltage, WFS, and TS will be considered as the independent variables. The range of the wire feed speed is 400-600 cm/min, the travel speed range is 12-18 cm/min, and the voltage range is 19-21 V. Welding parameters and their values are shown in Table 1.

Figure 1. Welding robot system in the experiment

Table 1. The GMAW process parameters

Parameter	Unit	Value
WFS	cm/min	400, 500, 600
TS	cm/min	12, 15, 18
Voltage	V	19, 20, 21
Gas flow rate	L/min	15
Weld bead length	mm	60

2.3 Experiment design

To find out the suitable parameter setting, an experi–ment design will be introduced, and the Taguchi method [4, 24, 25] will be applied. Three factors and three levels of parameters using the Taguchi method led to an L9 orthogonal matrix (as shown in Table 2), which can reduce the experimental demands significantly compa–red to the full factor experiment (27 experiments).

Table 2. L9 Taguchi design for 316L GMAW welding

Run	Voltage (volts)	WFS (cm/min)	TS (cm/min)
T1	1(19)	1(400)	1(12)
T2	1(19)	2(500)	2(15)
T3	1(19)	3(600)	3(18)
T4	2(20)	1(400)	2(15)
T5	2(20)	2(500)	3(18)
T6	2(20)	3(600)	1(12)
T7	3(21)	1(400)	3(18)
T8	3(21)	2(500)	1(12)
T9	3(21)	3(600)	2(15)

The macrostructure of the weld bead includes the appearance and geometry of the weld bead.

The geometry of the weld bead in terms of bead width, reinforcement, and penetration can be defined in the design stage and be measured and controlled throughout the process to achieve the required quality [26]. For this research, two values of the geometry will be measured as shown in Figure 2, which are the bead width (W) and reinforcement (R).

On the other hand, appearance determines whether the weld bead is even or not and whether there are surface defects, which will influence the AM products directly as, in AM processes, defects can accumulate layer by layer. In this research, one additional value for welding appearance will also be observed and valued.

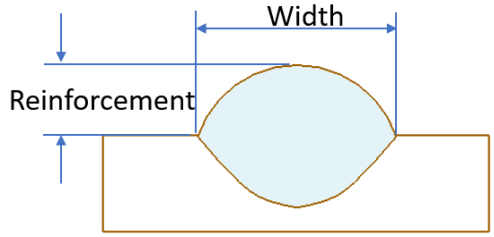

Figure 2. The geometry of a weld bead

3. RESULTS AND DISCUSSION

As mentioned above, the selected welding process parameters were varied at 3 levels. Therefore, 9 trials were welded, as shown in Figure 3. Related response values were measured (bead width and reinforcement) and calculated (aspect ratio of R/W) and discussed in the following sections.

3.1 Appearance observations

From the weld bead appearance observation, a good or bad quality weld bead can be decided in the first step. Generally, the surface should be smooth and free of any bumps, craters, or irregularities for a high-quality weld bead. This can also indicate whether the selection of the welding parameters is suitable. For example, in [27] bead flow, incomplete fusion of weld toe and hump, and scallop were defined as the factors to influence the welding appearance quality. All these factors could be obtained through observation.

One appearance value, value A (2 to 5), is intro–duced to evaluate the appearance, which is determined by the amount of welding spatter and welding bead uni–formity. For welding spatter in this study, there are three levels, which are no spatter (spatter value of 3 in Table 3), a small amount of spatter (spatter value of 2), and significant spatter (spatter value of 1). For welding bead uniformity, there are two levels, which are even bead and the bead with some wave and their value are 1 and 2 separately. Then, the sum of the spatter and uniformity values can be summed as the appearance value A.

The appearance of 316L welding beads using dif–ferent voltage, WFS, and TS are shown in Fig. 3. Wel–ding bead figures reveal that the application of different welding parameters can result in significant differences in the appearance of the welding start and end parts of the bead. There are more metal accu–mulations in welding start parts for T1, T3, T4, and T5, which may result in more severe metal accumulation in the multi-layer AM process, so their welding bead uniformity value will be lower. Although the welding start part for T8 has not presented much metal accumu–lation, the welding end is not smooth, so the uniformity value for this sample is still low. As mentioned above, the spat–ters will also be considered in this section because they will influence the welding quality, especially in the multi-layer AM process. The welding parameters can influence the spatter noticeably; as shown in Figure 3, there is no visible spatter in T2, T5, and T7, while T1, T3, and T6 have more spatters than other weld beads. All spatter and welding bead uni–formity values are lis–ted in Table 3, and these values will be applied as a reference when determining the optimal welding para–meters.

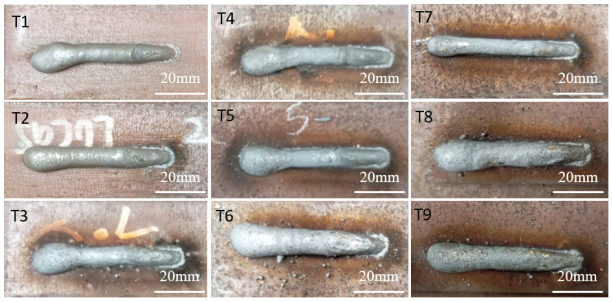

Figure 3. Welding bead appearance for 316L

Table 3. Spatter and welding bead uniformity values

Trials	Spatter	Welding bead uniformity	Overall Appearance value A
T1	2	1	3
T2	3	2	5
T3	1	1	2
T4	2	1	3
T5	2	1	3
T6	1	1	2
T7	1	2	3
T8	2	2	4
T9	1	2	3

3.2 Welding bead geometry

As mentioned above, reinforcement and width will be measured as responses and analyzed using the Taguchi method. Due to the metal accumulation at the welding start and metal lack at the welding bead end, the measurements will be carried out in the middle of the weld beads and average data for three sections of the weld beads are collected and shown in Table 4. The results revealed that the highest reinforcement is found for T6, which is 6.3 mm, and it is 43% higher than the lowest reinforcement from T7, which is 4.41 mm. The largest width is from T6, too, which is 8.84 mm, and it is about 55% higher than the lowest width from T7, which is 5.70 mm.

Both the highest reinforcement and width are from welding bead T6 and the lowest reinforcement and width are from welding bead T7, which means that the influence of different parameters on geometric dimen–sions follows certain trends. To find out the effects of

welding parameters on geometry, ANOVA and Taguchi method analysis will be applied using the data in Table 4. As per [28], the value of the aspect ratio was calcu–lated using the ratio of weld reinforcement to width (R/W), which is introduced as one value to determine if the parameters are fit for the application in additive manufacturing.

3.3 ANOVA for model responses

To validate the acceptability of the regression model of the Taguchi method application, Design Expert, version 22.0.8., [29] was utilized for the evaluation of the signifi–cance or non-significance of the models for selected respo–nses from ANOVA. A confidence level of 5% was set to determine the significance, which means that P-values less than 0.0500 indicate model terms are significant. In this section, the Predicted vs. Actual plots will be displayed to visualize the performance of a regression model.

Table 4. Widths and reinforcement for 316l with different voltage, WFS, and TS

Trials	Runs	Voltage (V)	WFS (cm/min)	TS (cm/min)	Reinforcement (mm)	Width (mm)	R/W
T1	1	19	400	12	5.8	7.16	0.81
T2	2	19	500	15	5.77	7.05	0.82
T3	3	19	600	18	5.5	6.92	0.79
T4	4	20	400	15	4.86	6.21	0.78
T5	5	20	500	18	4.61	6.48	0.71
T6	6	20	600	12	6.3	8.84	0.71
T7	7	21	400	18	4.41	5.7	0.77
T8	8	21	500	12	5.7	8.1	0.70
T9	9	21	600	15	5.88	8.21	0.72

(1) ANOVA for weld bead reinforcement

The statistical analysis of the regression model for the reinforcement is shown in Table 5. The P-value is 0.0267 which is less than 0.05, so the model terms are significant. It also shows that the F-value is 36.74, which also implies the model is significant, and there is only a 2.67% chance that an F-value this large could occur due to noise. The performance of this regression model can be visualized in the Predicted vs. Actual plot as shown in Figure 4, in which the actual sample points are close to the predicted model line. The fit statistics also indicated that this model can be used to navigate the design space.

Table 5. ANOVA for the selected factorial model for reinforcement

Source	Sum of Squares	df	Mean Square	F-value	p-value	
Model	3.33	6	0.5547	36.74	0.0267	Sig.
A-voltage	0.3443	2	0.1721	11.40	0.0806	
B-WFS	1.12	2	0.5614	37.18	0.0262	
C-TS	1.86	2	0.9306	61.63	0.0160	
Residual	0.0302	2	0.0151			
Cor Total	3.36	8				

Fit Statistics: R^2 = 99.10%; Adj. R^2 = 96.40%; Pred. R^2 = 81.79%

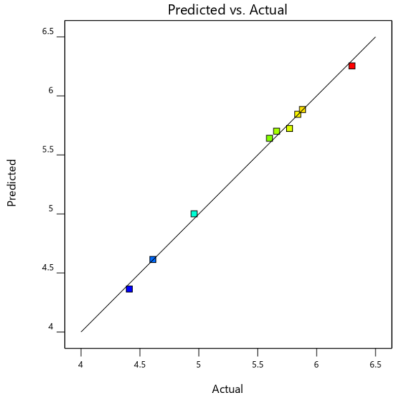

Figure 4. Predicted vs. actual plot for reinforcement

(2) ANOVA for weld bead width

The statistical analysis of the regression model for bead width is shown in Table 6. The P-value is 0.0230 which is less than 0.05, so the model terms are significant. It also shows that the F-value is 42.83, which implies the model is significant, and there is only a 2.30% chance that an F-value this large could occur due to noise. The performance of this regression model can be visualized in the Predicted vs. Actual plot as shown in Figure 5, in which the actual sample points are close to the predicted model line. The fit statistics also indicated that this model can be used.

Table 6. ANOVA for the selected factorial model for width

Source	Sum of Squares	df	Mean Square	F-value	p-value	
Model	8.30	6	1.38	42.83	0.0230	Sig.
A-voltage	0.1294	2	0.0647	2.00	0.0333	
B-WFS	4.00	2	2.00	61.97	0.0159	
C-TS	4.17	2	2.09	64.54	0.0153	
Residual	0.0646	2	0.0323			
Cor Total	8.37	8				

Fit Statistics: R^2 = 99.23%; Adj. R^2 = 96.91%; Pred. R^2 = 84.36%

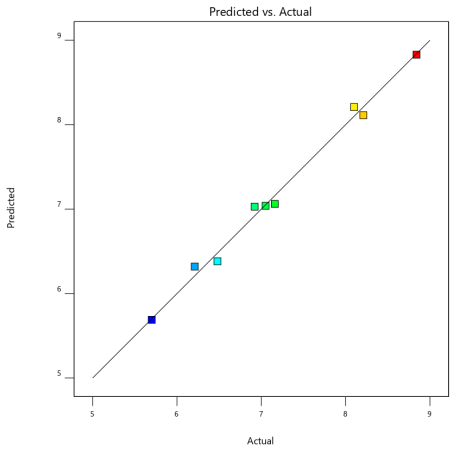

Figure 5. Predicted vs. actual plot for bead width

(3) ANOVA for aspect ratio R/W

The statistical analysis of the regression model for R/W is shown in Table 7. The P-value is 0.0489 which is less than 0.05, so the model terms are significant. It also shows that the F-value is 19.77, which implies the model is significant, and there is only a 4.89% chance that an F-value this large could occur due to noise. The performance of this regression model can be visualized in the Predicted vs. Actual plot as shown in Figure 6, in which the actual sample points are close to the predicted model line, and as for reinforcement and width, the statistics also indicated that this model can be used.

Table 7. ANOVA for the selected factorial model for R/W

Source	Sum of Squares	df	Mean Square	F-value	p-value	
Model	0.0171	6	0.0029	19.77	0.0489	Sig.
A-voltage	0.0124	2	0.0062	43.00	0.0227	
B-WFS	0.0030	2	0.0015	10.23	0.0890	
C-TS	0.0018	2	0.0009	6.08	0.1413	
Residual	0.0003	2	0.0001			
Cor Total	0.0174	8				

Fit Statistics: R^2 = 92.47%; Adj. R^2 = 93.37%; Pred. R^2 = 66.42%

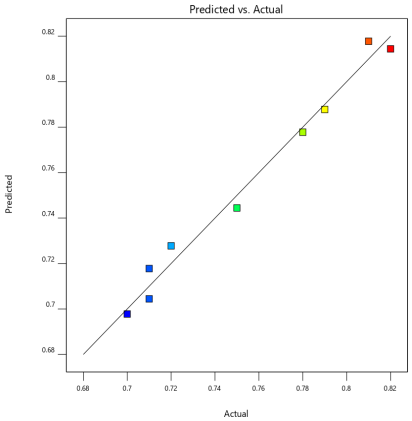

Figure 6. Predicted vs. actual plot for respect ratio R/W

3.4 Taguchi Method Application

Taguchi method applications are based on the data in Table 3, where reinforcement, width, and aspect ratio R/W are treated as the response values. The main effect plots for reinforcement, width and appearance using different welding parameters (Voltage, WFS, and TS) are shown in Figure 7 to Figure 9 separately. From these plots, the influence of each independent parameter on the response can be obtained.

(1) Reinforcement

As shown in Figure 7 the reinforcements of the weld beads increase when WFS increasing, because with a higher WFS more materials can enter form the wire feeder to the nozzle to melt and deposited on the bead [30]. More material deposition will lead to metal accumulation and a larger height. The negative influence of TS is significant as shown in Figure 7 too, which means that with the increase of TS the reinforcement decreases because the a higher speed of the torch will limit the deposition time on the weld bead then lead to less metal accumulation on the bead surface [31]. The effect of voltage on reinforcement shows that with the voltage increasing, the reinfor–cement decreases slightly.

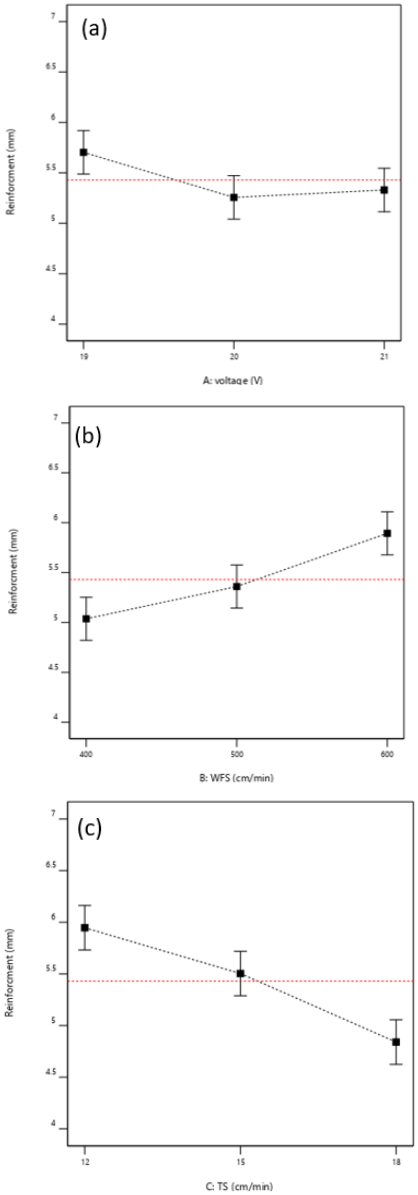

Figure 7. Main effects plot for reinforcement, (a) Voltage, (b) WFS, and (c) TS

The relationship between parameters and responses can be judged more clearly in rank order, which reveals the most important/effective input on output.

Table 8. Response table for mean effects of reinforcement

Level	Voltage	WFS	TS
1	5.723	5.057	5.947
2	5.317	5.347	5.537
3	5.317	5.953	4.873
Delta	0.407	0.897	1.073
Rank	3	2	1

As shown in Table 8, TS is the rank 1 of the three parameters, which means that the reinforcement can be influenced by TS significantly, then followed by WFS and Voltage. Looking just at the reinforcement requirement, lower TS, higher WFS, and lower Voltage should be considered.

(2) Bead width

From the purpose of the AM process, lower bead width has positive effects on the manufacturing process, so lower bead width will be treated as the objective in this section. As shown in Figure 8 the widths of the weld beads increase when WFS increases, as a similar reason for reinforcement, because a higher WFS can allow more material to enter from the wire feeder to the nozzle to be melted and deposited on the bead. More material deposition will lead to metal accumulation and enlarge the bead widths. A declining trend of widths is signi–ficant when TS is increasing, as shown in Figure 8, which means that with the increase of TS, the bead width decreases because a higher speed of the torch will limit the deposition time than less metal accumulation on the bead surface. The effect of the voltage shows a substantial trend for bead widths, the lower voltage will result with the lower bead width.

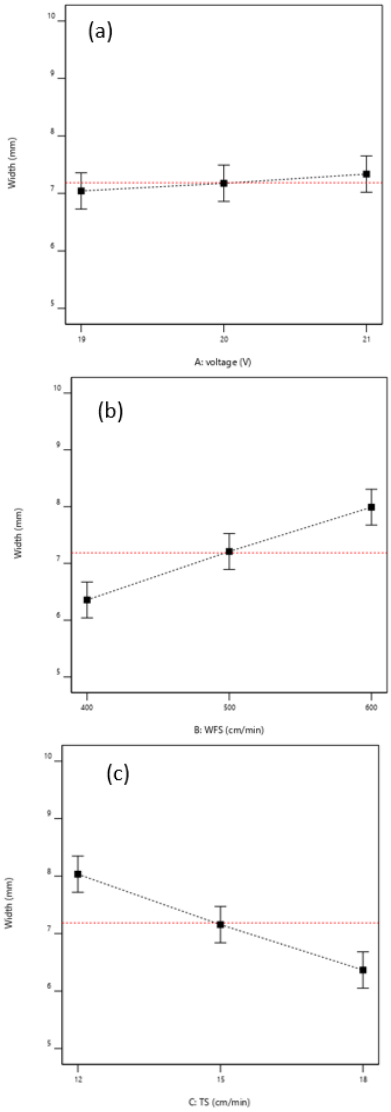

Figure 8. Main effects plot for bead width, (a) Voltage, (b) WFS, and (c) TS

As shown in Table 9, the response table for means of width reveals that the rank order is the same as for the reinforcement, the first one is TS followed by the WFT and Voltage. To get a lower width, higher TS, lower WFS, and lower voltage should be considered in turn.

Table 9. Response table for mean effects of bead width

Level	Voltage	WFS	TS
1	7.043	6.323	8.230
2	7.143	7.407	7.123
3	7.533	7.990	6.367
Delta	0.490	1.667	1.863
Rank	3	2	1

(3) Aspect ratio (R/W)

The R/W value is calculated from the values of reinforcement and bead width, it can indicate the relationship between the two responses. As shown in Figure 9 with the increase of voltage and WFS the value of R/W decreases slightly, which means that when voltage and WFS increase the material expansion horizontal (bead width) is larger than the deposition in vertical direction(reinforcement). Figure 9c shows that there is a maximum value of R/W, which means that using the TS of 15 cm/min the related value of reinforcement increasing is higher than the related value of bead width increasing.

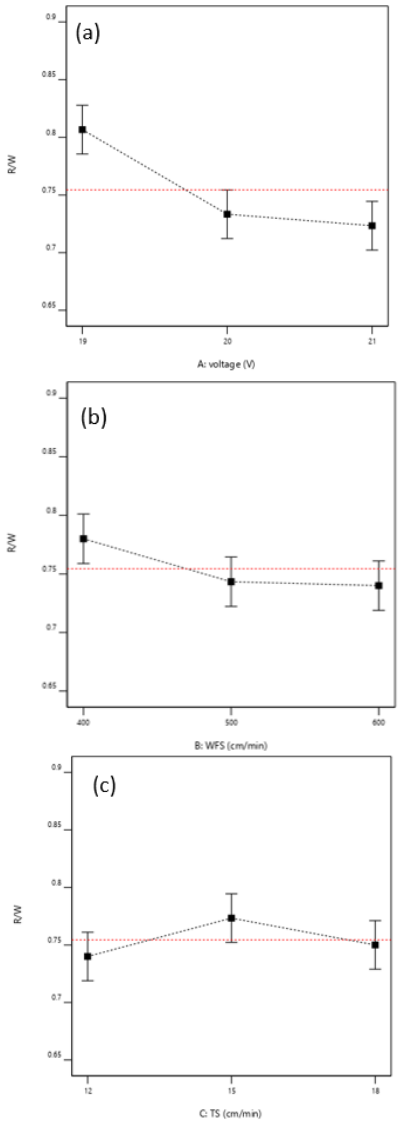

Figure 9. Main effects plot for R/W, (a) Voltage, (b) WFS, and (c) TS

From the rank order in Table 10 and the main effects plot in Figure 9, the voltage has the highest rank order,

which means that this parameter can influence the R/W more significantly than WFS and TS. Lower voltage can obtain higher R/W, so 19 V leads to the highest R/W in this range.

Table 10. Response Table for Mean effects of R/W

Level	Voltage	WFS	TS
1	0.8133	0.8000	0.7267
2	0.7467	0.7267	0.7833
3	0.7167	0.7500	0.7667
Delta	0.0967	0.0733	0.0567
Rank	1	2	3

The Taguchi method application results, from Figure 7a, Figure 8a, and Figure 9a, show that to get higher reinforcement, lower width and higher R/W, the lower voltage should be selected, which is 19 V. There are conflicts in the selection of WSF and TS for the above aims. For example, for lower WFS welding, both the higher bead width and higher reinforcement will be obtained. So the R/W value is considered as the criteria for optimization. As shown in Table 4, when the voltage is 19 V, the R/W of T1, T2 and T3 are 0.81, 0.82 and 0.79, which are the top three among the all value. The values are close to each other, so bead appearance value (in Table 3) is applied as the reference value, which indicates that T2 has a much higher value than the other two, so parameters for T2 can be considered as the optimal parameters, which are voltage of 19 V, WFS of 500 cm/min and TS of 15 cm/min.

4. FULL FACTORIAL DESIGN OF EXPERIMENT AND APPLICATION

4.1 Full factorial optimization

As shown above, the best parameters are voltage of 19 V, WFS of 500 cm/min, and TS of 15 cm/min. In order to get more optimal WFS and TS parameters and investigate the interaction between parameters, a smaller gap between the two parameters is introduced. Two factors (WFS and TS), on three levels of full factorial design are shown in Table 11 WFS ranges from 450 cm/min to 550 cm/min and TS from 13.5 cm/min to 16.5 cm/min are applied.

Table 11. Reinforcement and width for the full factorial design of the experiment

Trails	WFS (cm/min)	TS (cm/min)	Reinforcement (mm)	Width (mm)	R/W
F1	450	13.5	5.35	7.44	0.72
F2	450	15	5.3	6.75	0.79
F3	450	16.5	5.25	6.7	0.78
F4	500	13.5	5.6	8.19	0.68
F5	500	15	5.70	7.11	0.80
F6	500	16.5	5.5	7.18	0.77
F7	550	13.5	5.76	8.7	0.66
F8	550	15	5.67	8.15	0.70
F9	550	16.5	5.47	7.46	0.73

In this section, appearance value A will not be considered, because as shown in Figure 10, there is no visible spatter under the parameters in this range, and the uniformity of the welding beads is kept in an acceptable range.

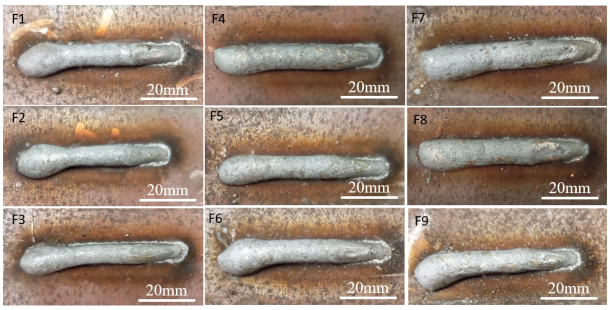

Figure 10. The weld bead for full factorial design

As mentioned above the reinforcement and the width value are both average value for three-time measu–rements. The data in Table 11 has the same trends obta–ined using Taguchi method. It also revealed that under the same WFS higher TS will lead to lower rein–forcement and width, while when using the same TS, higher WFS will lead to higher reinforcement and width.

For further study, the interaction of WFS and TS, namely WFS*TS is considered, and the interaction has been shown in Figure 11. It revealed that in WFS of 500 cm/min, the green line (TS of 15 cm/min) has the highest value for reinforcements, the highest R/W and lower width.

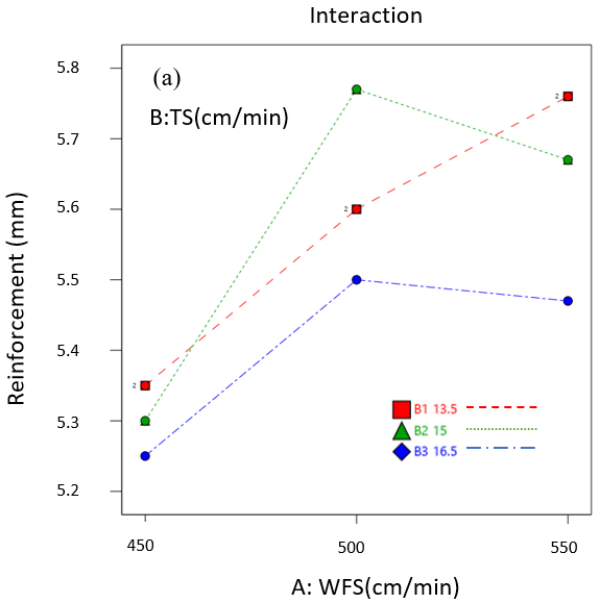

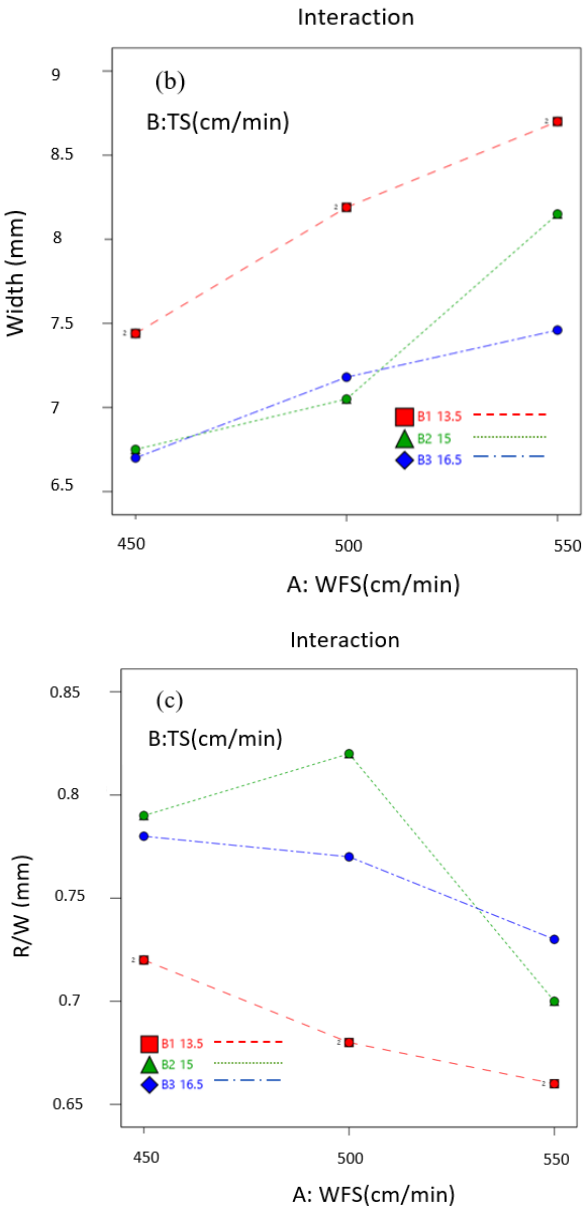

Figure 11. Interaction of WFS and TS for reinforcement (a), bead width (b) and R/W (c)

4.2 Application in multilayer AM process

Optimal welding parameters (Voltage of 19 V, WFS of 500 cm/min, and TS of 15 cm/min) from the above study were applied as the GMAW AM parameters. 120s was selected as the dwell time for interlayer cooling, which helps the part to cool down for the next deposition. As shown in Figure 12 the multi-layer single pass 316L wall has a good appearance, especially the first 12 layers. From the 13th layer (as shown in Figure 12), there is visible melt flow from the upper layers to the lower layers, which can influence the surface waviness significantly. It is assumed that the unevenness is caused by the higher temperature from the previous layers when deposition of the next layer starts. So, the dwelling time strategy will be considered for the next trial.

It was also observed that the surface of the part structure is smooth, the distance between each layer is equal, the connections between layers are tight, and there are no gaps. There was minimal spattering occurring during the welding, indicating that the parameters were stable during the entire welding process. This time, 20 layers were welded, the total height was 65 mm, and the average height of each layer was 3.25 mm. This height can ensure high welding efficiency. Therefore, the welding parameters optimized in this article can be applied to the subsequent 316L stainless steel additive manufacturing process to ensure a better-forming appearance and higher deposition efficiency.

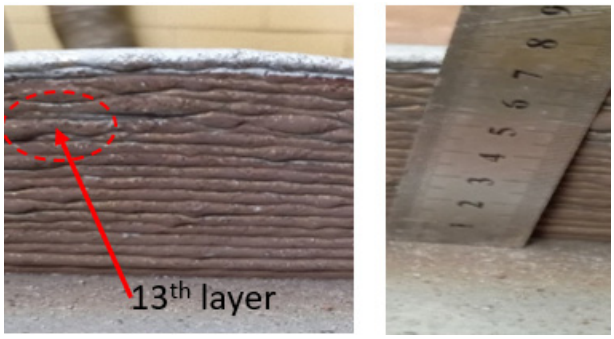

Figure 12. Appearance of 20 layers single pass wall for 316L

5. CONCLUSION

The preliminary experiment of welding parameters for better appearance, higher reinforcement, and lower width are carried for the future GMAW AM process because single-layer weld beads can influence the multilayer structures directly. Taguchi method and full factorial design were employed, and the main conclusions are shown below.

(1) Spatter and uniformity were employed to evaluate the appearance of the weld beads. No visible trends for the effects of different parameters on the appearance were observed, which means that appearance is not influenced by individual parameters, but by the interaction and combination of various parameters.

(2) ANOVA showed the statistical significance for both reinforcement, width, and respect ratio R/W of the mean square model.

(3) Voltage is the least important factor for reinforcement and bead width, but it is the most important for R/W. With its increase the reinforcement and the width increase, while the R/W value decreases.

(4) TS is the most important factor for reinforcement and bead width, it can reduce the reinforcement and width when it increases. The lowest reinforcement and width are found for TS of 18 cm/min.

(5) Higher WFS intends to higher reinforcement and width and the highest reinforcement and width are found for WFS of 600 cm/min.

(6) Full factorial design was carried out based on the Taguchi method analysis and with the more refined experiment parameters. The result verified the optimal parameters scheme, voltage of 19 V, WFS of 500 cm/min, and TS of 15 cm/min is the optimization.

(7) The multilayer single-pass AM structure was obtained using the optimal parameters and the appearance and geometry show its reliability.

The results from this study can be applied to future AM processes for higher efficiency and better surface quality. Moreover, the combination of the Taguchi method and the full factorial method can be treated as a suitable method to get the optimal results.

For future study, processing parameters dwelling time will be optimized for additive manufacturing to obtain good appearance, properties, and manufacturing efficiency.

REFERENCE

[1] Chen, X.X. et al., A Review of the Development Status of Wire Arc Additive Manufacturing Technology, Advances in Materials Science and Engineering, Vol. 2022, 2022.

[2] ASTM-International, ISO/ASTM52900-15 Standard Terminology for Additive Manufacturing General Principles - Terminology. ASTM-International: West Conshohocken, 2016.

[3] Citarella, R., Giannella, V., Additive Manufacturing in Industry, Applied Sciences-Basel, Vol. 11, No. 2, 2021.

[4] Güden, S., Motorcu, A.R., Yazici, M., Examining and Optimizing the Weld Area and Mechanical Performance of Thermoplastic Parts Manufactured by Additive Manufacturing and Welded by Friction Stir Welding, FME Transactions, Vol. 52, No. 2, pp. 279-294, 2024.

[5] Bártová, K., Bárta, J. and Ptačinová, J., Study of Multilayer Welded Structure Made of AISI 316LSi Using WAAM. Tehnicki vjesnik-Technical Gazette, Vol. 31, No 2, pp. 574-578. 2024.

[6] Radojičić, S., Konjatić, P., Katinić, M. Kačmarčik, J., The Influence of Material Storage on Mechanical Properties and Deterioration of Composite Materials. Tehnicki vjesnik-Technical Gazette, Vol. 30, No. 5, pp. 1645-1651. 2023.

[7] Vrancken, B. et al., Heat treatment of Ti6Al4V produced by Selective Laser Melting: Microstructure and mechanical properties, Journal of Alloys and Compounds, Vol. 541, pp. 177-185, 2012.

[8] Xia, C.Y. et al., A review on wire arc additive manufacturing: Monitoring, control and a framework of automated system, Journal of Manufacturing Systems, Vol. 57, pp. 31-45, 2020.

[9] Zahidin, M.R. et al., Research challenges, quality control and monitoring strategy for Wire Arc Additive Manufacturing, Journal of Materials Research and Technology-Jmr&T, Vol. 24, pp. 2769-2794, 2023.

[10] Sinha, A.K., Pramanik, S. Yagati, K.P., Research progress in arc based additive manufacturing of aluminium alloys - A review, Measurement, Vol. 200, 2022.

[11] Chaudhari, R. et al., A parametric study and experimental investigations of microstructure and mechanical properties of multi-layered structure of metal core wire using wire arc additive manufacturing, Journal of Advanced Joining Processes, Vol. 8, 2023.

[12] Jin, W.W. et al., Wire Arc Additive Manufacturing of Stainless Steels: A Review, Applied Sciences-Basel, Vol. 10, No. 5, 2020.

[13] Vora, J. et al., Optimization of Bead Morphology for GMAW-Based Wire-Arc Additive Manufacturing of 2.25 Cr-1.0 Mo Steel Using Metal-Cored Wires, Applied Sciences-Basel, Vol. 12, No. 10, 2022.

[14] Zhao, Y.T., Li, W.G., Liu, A., Optimization of geometry quality model for wire and arc additive manufacture based on adaptive multi-objective grey wolf algorithm, Soft Computing, Vol. 24, No. 22, pp. 17401-17416, 2020.

[15] Long, P., *Microstructure and Properties of 316L Stainless Steel Fabricated by Wire Arc Additive Manufacturing*, Huazhong University of Science &Technology, 2020.

[16] Ekaputra, I.M.W., Gunawan Dwi Haryadi, S.M., Dewa, R.T., Kim, S.-J., The influence of welding speed conditions of GMAW on mechanical properties of 316L austenitic stainless steel. in: *The 2nd International Joint Conference on Advanced Engineering and Technology (IJCAET 2017) and International Symposium on Advanced Mechanical and Power Engineering (ISAMPE 2017)*, 2018.

[17] Saha, M.K.H., Ritesh, Ajit, M., Santanu, D., Effect of Heat Input on Geometry of Austenitic Stainless Steel Weld Bead on Low Carbon Steel, Journal of the Institution of Engineers (India) Series C, Vol. 100, No. 4, pp. 607-615, 2019.

[18] Chaudhari, R. et al., Parametric Study and Investigations of Bead Geometries of GMAW-Based Wire -Arc Additive Manufacturing of 316L Stainless Steels, Metals, Vol. 12, No. 7, 2022.

[19] Vora, J. et al., Experimental investigations on mechanical properties of multi-layered structure fabricated by GMAW-based WAAM of SS316L, Journal of Materials Research and Technology-Jmr&T, Vol. 20, pp. 2748-2757, 2022.

[20] Yao, P. et al., Influence of Inclination of Welding Torch on Weld Bead during Pulsed-GMAW Process, Materials, Vol. 13, No. 11, 2020.

[21] Kumar, A. Maji, K., Selection of Process Parameters for Near-Net Shape Deposition in Wire Arc Additive Manufacturing by Genetic Algorithm, Journal of Materials Engineering and Performance, Vol. 29, No. 5, pp. 3334-3352, 2020.

[22] Xu, S.H., Wang, Y.D., Estimating the effects of corrosion pits on the fatigue life of steel plate based on the 3D profile, International Journal of Fatigue, Vol. 72, pp. 27-41, 2015.

[23] Wu, W. et al., Forming Process, Microstructure, and Mechanical Properties of Thin-Walled 316L Stainless Steel Using Speed-Cold-Welding Additive Manufacturing, Metals, Vol. 9, No. 1, 2019.

[24] Nobrega, G. et al., Parametric Optimization of the GMAW Welding Process in Thin Thickness of Austenitic Stainless Steel by Taguchi Method, Applied Sciences-Basel, Vol. 11, No. 18, 2021.

[25] Ram, J.S., Shiek, J., Syed, S.H., Multi-response Optimization of PMEDM on Inconel 718 Using Hybrid T-GRA TOPSIS, and ANN Model, FME Transactions, Vol. 51, No. 4, pp. 564-574, 2023.

[26] Bestard, G.A. and Alfaro, S.C.A., Measurement and estimation of the weld bead geometry in arc welding processes: the last 50 years of development, Journal of the Brazilian Society of Mechanical Sciences and Engineering, Vol. 40, No. 9, 2018.

[27] Xiong, J., Zhang, G.J. and Zhang, W.H., Forming appearance analysis in multi-layer single-pass GMAW-based additive manufacturing, International Journal of Advanced Manufacturing Technology, Vol. 80, No. 9-12, pp. 1767-1776, 2015.

[28] Sathishkumar, M. et al., Effect of Welding Speed on Aspect Ratio of Hastelloy X Weldment by Keyhole Plasma Arc Welding (K-PAW), Materials Today-Proceedings, Vol. 22, pp. 3297-3304, 2020.

[29] Design Expert, version 22.0.8., Stat-Ease, Inc., 2023.

[30] Kumar, V. et al., Parametric study and characterization of wire arc additive manufactured steel structures, International Journal of Advanced Manufacturing Technology, Vol. 115, No. 5-6, pp. 1723-1733, 2021.

[31] Zhou, Y.H. et al., Influence of travel speed on microstructure and mechanical properties of wire plus arc additively manufactured 2219 aluminum alloy, Journal of Materials Science & Technology, Vol. 37, pp. 143-153, 2020.

NOMENCLATURE

AM	additive manufacturing
BBD	Box-Behnken design
BH	bead height
BW	bead width
DOE	design of experiment
GMAW	gas metal arc welding
MOTLBO	multi-objective teaching-learning-based optimization
R	reinforcement
R/W	ratio of weld reinforcement to width
TS	travel speed
W	width
WAAM	wire + arc additive manufacturing
WFS	wire feed speed
WM	weld metal zone

ПРЕЛИМИНАРНА СТУДИЈА ГЕОМЕТРИЈЕ НАВАРА КОД НАВАРИВАЊА НА НЕХРЂАЈУЋИ ЧЕЛИК 316Л КОРИШТЕЊЕМ МИГ ПОСТУПКА ЗАВАРИВАЊА

Х. Ванг, Ш. Кларић, С. Хаврлишан

Примјеном поступка електролучног заваривања таљивом електродом у заштити инертног гаса (МИГ) могу се произвести метални делови у адитивној производњи (ап) јер овај поступак има предности у виду брже производње и уштеде материјала. Међутим, постоје различити захтеви за наваре код примене МИГ поступка у адитивној производњи у поређењу с конвенционалним заваривањем те је спроведено прелиминарно истраживање МИГ поступка на нерђајућем челику 316Л како би се пронашли оптимални параметри напона, брзине додавања жице (БДЖ) и брзине заваривања (БЗ). Тагучи метода коришћена је како би се добили параметри за постизање жељеног надвишења навара, мање ширине те већег односа ширине и надишења навара (p/w). Оптимални параметри, добијени међу узорцима су: напон 19 V, БДЖ 500 cm/min и БЗ 15 cm/min. како би се додатно истражио утицај тих параметара и потврдили резултати, спроведен је потпуни факторски план експеримента с два фактора на три висине, узимајући у обзир интеракцију између фактора. На крају су испитани параметри примењени у адитивној производњи применом роботизованог МИГ поступка заваривања како би се проверила њихова поузданост.